14th IEA Heat Pump Conference
15-18 May 2023, Chicago, Illinois

Analysis of Large-Scale Ammonia Heat Pumps in Transient Operating Conditions

Kenneth Rugholm Kramer [a], Jonas Lundsted Poulsen [a,*], Wiebke Meesenburg [b], Mathias Kjær Christensen [c], Peter Reinholdt [c], Brian Elmegaard [b], Benjamin Zühlsdorf [a]

[a]*Danish Technological Institute, Energy and Climate, Aarhus, Denmark*
[b]*Technical University of Denmark, Department of Civil and Mechanical Engineering, Kgs. Lyngby, Denmark*
[c]*Johnson Controls Denmark ApS, Holme, Denmark*

Abstract

Large-scale ammonia heat pumps are a key technology for enabling sustainable heat supply. Exploiting their potential in integrated systems requires the highest efficiencies and reliability even at varying operating conditions. The varying operating conditions can result from variations in the heat source and sink, such as variations in production processes and sudden changes of weather conditions. The dynamic operating conditions may result in unwanted dynamic effects, risking sub-optimal performance and component damage. This study focuses on the development and validation of dynamic models for the components in an ammonia heat pump system. The various components were assembled in a dynamic model implemented in Dymola and validated against test data from operation of a MW-scale ammonia heat pump. The system responses to sudden changes in the source and sink conditions, compressor speed, and liquid levels in the system were studied. The results from the validation showed that this dynamic model has great potential to be used for developing holistic control strategies and design guidelines in order to further improve the resilience and performance under fluctuating boundary conditions for large-scale heat pumps.

Selection and/or peer-review under the responsibility of the organizers of the 14th IEA Heat Pump Conference 2023.

Keywords: Large-scale heat pump; Dynamic model; Experimental validation; Control; Dymola

1. Introduction

Large-scale heat pumps are key components for the decarbonization of district heating and industrial heat supply. In line with the efforts to reduce greenhouse gas emissions from the heating sector, the number of installed large-scale and domestic heat pumps is increasing rapidly worldwide [1]. Large-scale heat pumps integrated with ambient heat sources or industrial processes may be required to operate under variable boundary conditions such as rapid changes in the sink or source temperature or flow. These may e.g. occur due to rapid changes in the outdoor air conditions for air-source heat pumps or due to variations related to the type of industrial process the heat pump is supplying heating (and cooling) to. If the systems is not designed to be able to handle such variations, the rapid change in boundary conditions may lead to unwanted dynamic effects, risking sub-optimal performance and component damages [2].

Designing large-scale heat pumps and the respective control systems to operate optimally under expectable and unforeseen variations in the boundary conditions requires studying the dynamic response of the system to such variations. This may be done using validated dynamic models of the system that are based on fundamental physics and thereby applicable to a broad range of operation conditions. Using models to test the dynamic response of the system to different variations in the boundary conditions is expected to reduce costs and time for testing and to reduce the risk of harming the experimental set-up if too extreme variations are tested. Such

*Corresponding author. Tel: +45 72201378
E-mail address: jlp@teknologisk.dk

models form the basis for tasks such as analysis of system behaviour, system design, model based control design, controller tuning and fault detection and diagnosis [3]. Li et al. provide an extensive overview of the common practices of dynamic modelling of HVAC systems [4-5]. These include component based modelling and the use of the object-oriented programming language Modelica [6] for the implementation, which has been shown to be a suitable approach [7].

This approach has previously been applied to large-scale ammonia heat pumps to assess the ability of large scale heat pumps to supply frequency regulation service to the electricity grid [8]. The same dynamic model was used to assess which components in a two-stage heat pump system have the largest influence on the time constant for changing the load in large-scale heat pumps [9]. Recent studies on large-scale heat pumps used dynamic models to optimize the controller set-points [10] and assess the influence of heat exchanger fouling [11].

The present study aimed to develop and validate a dynamic model for a MW-scale single-stage ammonia heat pump system using a screw compressor and flooded evaporator. The models were developed based on the underlying physics, fitted against design data of the individual components, and validated against measurement data. The available measurement data was obtained from experiments, in which different controller set-points were changed to excite the system. The model was used to analyze the dynamic response of the system to the changes in set-points such as compressors speed, receiver level, sink/source temperature and flow variations. The intended future use of the model is to use it for optimization of both the design and the control of similar large-scale systems to ensure optimal performance during rapidly changing boundary conditions.

2. Methods

2.1. Case description

Fig. 1 shows the overall heat pump cycle layout and control dependencies for the main components as well as the independent input parameters used in the model.

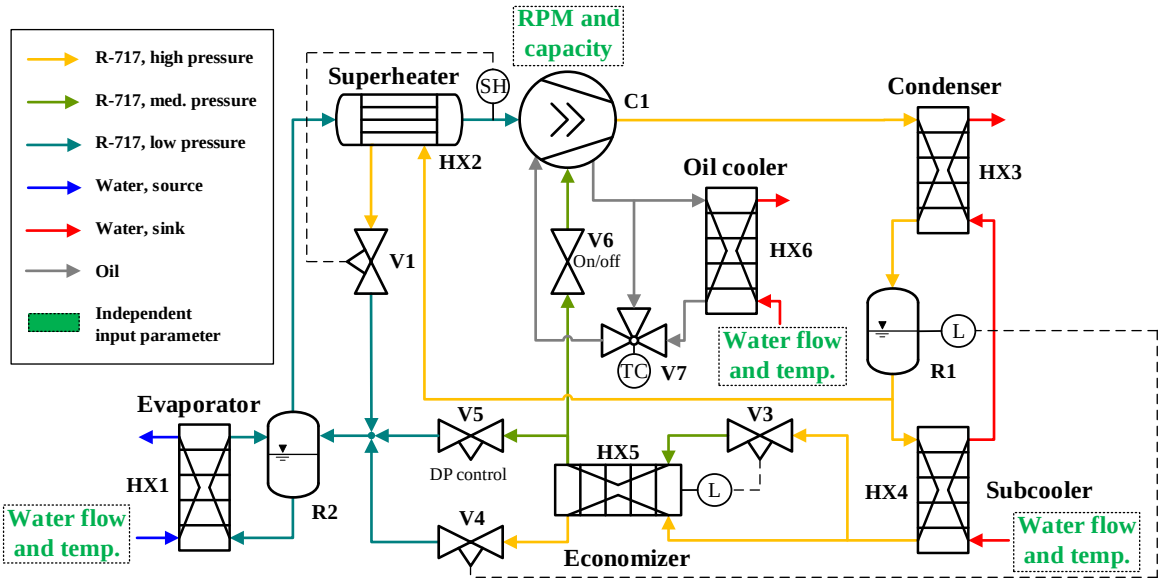

Fig. 1. Layout of heat pump system, including independent input parameters (written in green).

The heat pump consists of the following main components; screw compressor (C1), plate oil-cooler (HX6), plate condenser (HX3), liquid separators (R1 and R2), plate-and-shell sub-cooler (HX4), plate-and-shell economizer (HX5), plate evaporator (HX1), shell-and-tube superheater (HX2), and expansion valve (V4). The controllers modelled included:

- Receiver (R1) level controlled by main expansion valve (V4).
- Economizer (HX5) liquid level controlled by economizer valve (V3).
- Suction gas superheating (HX2) controlled by valve on the liquid side (V1).
- On/off control valve (V6) and differential pressure valve (V5) for economizer gas flow.
- Inlet temperature of oil to the compressor (C1) controlled by 3-way valve (V7).

To validate the dynamic model and compare it with the operating data from the heat pump, it was necessary to have identical boundary conditions between the model and measured data. For this, various independent parameters were used, which were variable inputs to the heat pump. In Fig. 1 these inputs are highlighted in green and consist of input temperatures and flows on the water side of the sub-cooler, oil-cooler, evaporator, as well as the compressor speed and capacity.

The dynamic model of the heat pump was developed in Dymola [12] with the component library TIL suite [13], based on the object-oriented language Modelica [14]. The basis of the dynamic system model was individual component models, which were first developed, tested, and validated against design data before the component models were assembled in the system model. Both the components and the system were modelled based on a finite volume method [15], consisting of mass, energy and momentum balances supplemented with semi-empirical correlations for describing the component characteristics. The process of preparing the validated dynamic model can be seen in Fig. 2. In step 1 (component modelling) the various component models were first developed by inserting relevant parameters for the available data, e.g. material type and geometry specifications for the heat exchangers. After this, other parameters such as e.g. the heat transfer coefficients and pressure loss coefficients were fitted against data available from standard calculations from e.g. manufacturer component design software, data sheets or experiments. In step 2 (system modelling) the component models were assembled in a system model and the control parameters were defined. Finally, in step 3 (validation) the model was validated by comparing the model results with measurement data from experiments with the heat pump system. The modelling process (step 1 to 3) was iterated where needed. Hence, independent datasets have been used for fitting (component design data) and validation (measurement data from experiments) to develop the final system model.

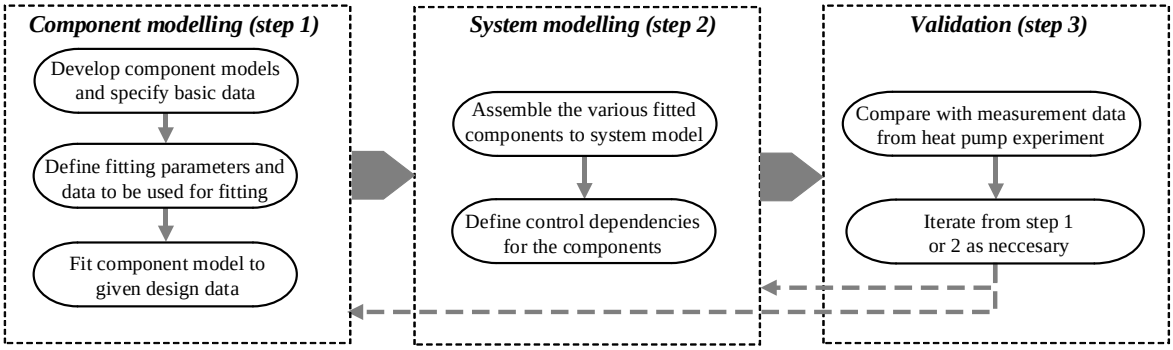

Fig. 2. Illustration for the process in relation to the development of the dynamic model.

Coefficients for the different component models from the TIL component library were fitted in relation to, for example, heat transfer, pressure loss, and friction to match the associated design points in the given component. Examples of the component modelling for the heat exchangers and the compressor are given in the following two sections.

2.2. Heat Exchangers

The heat pump consisted of six heat exchangers of different types and sizes. The three plate heat exchangers are standard components in the TIL suite component library, while the two plate-and-shell heat exchangers and the one shell-and-tube heat exchanger were modelled to be compatible with TIL suite. For all the heat exchangers, the geometry was known, and the models were based on this information. All the heat exchangers were fitted in relation to a series of different design conditions and compared with the heat transfer rate (HTR), outlet temperatures and pressure drops using TLK's Modelfitter tool [16]**.** In addition, pressure loss correlations based on [16,17,18] were used. The fitting procedure used for the evaporator is used as an example of the fitting process.

The model of the evaporator which is a large plate heat exchanger was discretized into 10 cells on the water and ammonia side, respectively. On the water side, a constant heat transfer coefficient was fitted, while on the ammonia side, a heat transfer model was used [20] which was subsequently fitted with a correction factor and a reference heat transfer coefficient. To compare and fit the model against the component design data, a virtual test bench of the component model in Dymola was converted according to the Functional Mock-up Interface standard [21], see Fig. 3, and fitted in TLK's Modelfitter tool. Here, different various independent parameters (input parameters) for the component were inserted and the dependent parameters for the model and design data were compared. For the heat exchanger, five independent parameters were used: enthalpy, mass flow, and pressure of ammonia, and the flow and temperature of water, see Fig. 3.

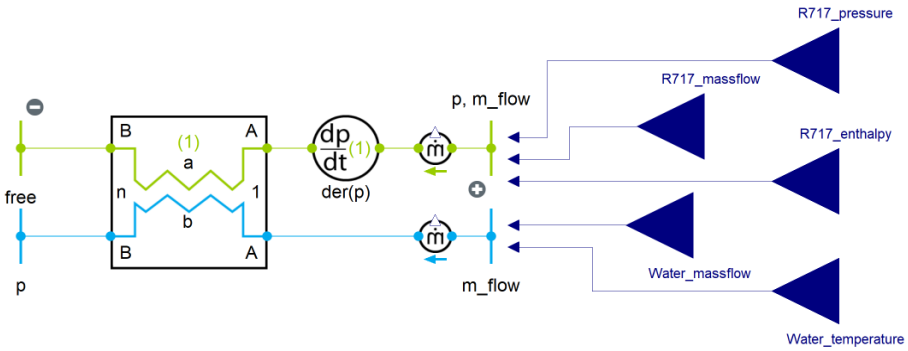

Fig. 3. Content of Functional Mock-up Unit for virtual test bench for model of evaporator plate heat exchanger.

Fig. 4 shows three different dependent parameters for nine different steady-state design points from the manufacturer component design software: heat transfer rate, water temperature out and pressure drop on the ammonia side. The difference between model and design points for the evaporator before and after the fit is shown, and it can be seen the R^2 score was satisfactorily high after fitting.

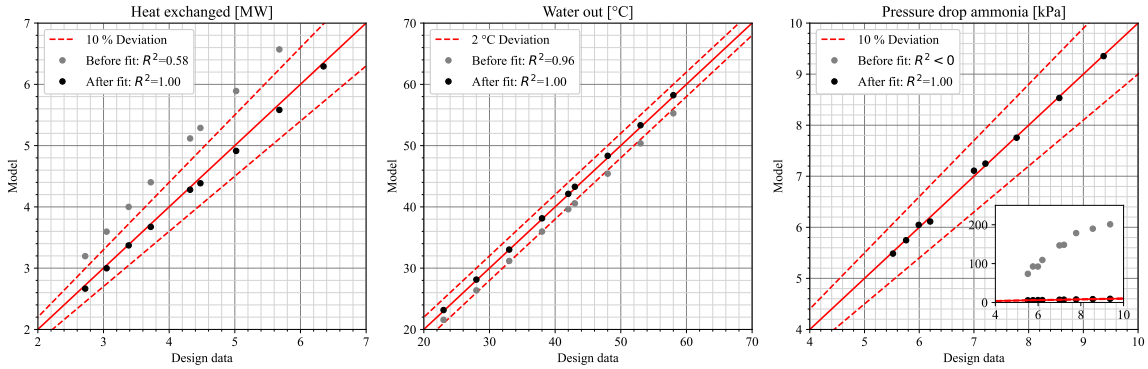

Fig. 4. Differences between mode and design data before and after fitting of evaporator.

2.3. Screw Compressor

The model for the screw compressor was based on the compressor base classes from the TIL suite library [13], but some extra functionalities were added to the model in order for it to include the principles of the modelled heat pump. This included among other things an automatically regulating volume ratio within a predefined interval, a capacity slide valve control, and oil cooling. The model was divided in three volumes (inlet, outlet, and economizer volume) and for each volume dynamic mass and energy conservation equations were implemented. Fig. 5 shows how the different control volumes were connected to each other.

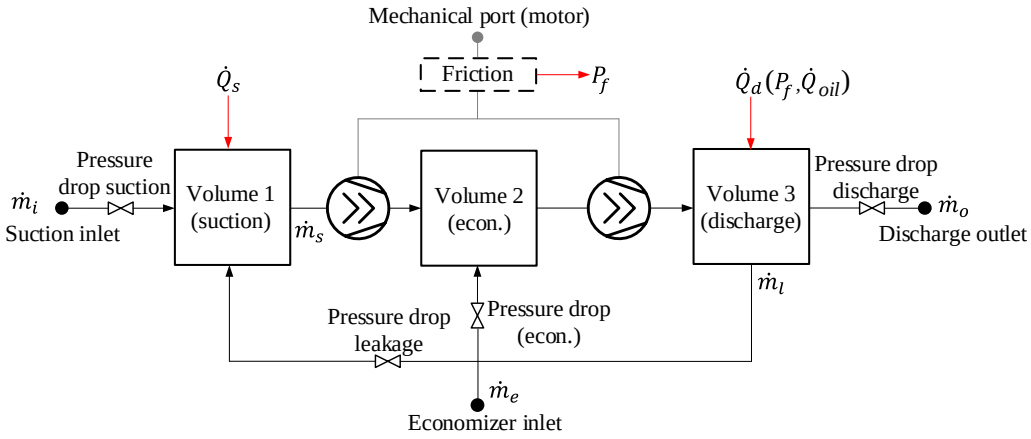

Fig. 5. Modelling of screw compressor with injection from economizer port (adapted from [22]).

The energy balance for the suction and discharge volume were influenced by $\dot{Q}_s$ and $\dot{Q}_d$, respectively. For the discharge volume, $\dot{Q}_d$ was calculated based on the friction power, P_f, which was a function of the compressor RPM, two empirical friction coefficients, and the torque. Furthermore, oil cooling ($\dot{Q}_{oil}$) was modeled and applied in the discharge volume only and thus also a part of $\dot{Q}_d$. The modeling of the oil cooling was based on a dynamic balance equation and formulated independently of the refrigerant volume. In this way, only heat was exchanged between the oil and the refrigerant. In addition, the liquid oil was assumed incompressible (simplified energy balances).

Several steady-state design data points from the compressor were used to fit the screw compressor, e.g. by varying the friction coefficients and cross-sectional areas for the valve areas determining the flow rates with the use of the Saint-Venant and Wantzel equation [23].

The automatic regulating volume ratio and the oil flow were determined using a polynomial fit based on steady-state design data of the screw compressor and were then used in the model to determine the volume ratio and the oil flow. The design data were generated for all combinations of evaporating temperatures in the range of 20 °C to 45 °C and condensing temperatures in the range 65 °C to 95 °C with a 5 °C resolution at 3600 RPM. Fig. 6 shows a comparison of the design data and the respective fits for oil flow and volume ratio. The oil flow polynomial fit was made as a function of the pressure difference, while the volume ratio polynomial fit was made as a function of the pressure ratio, compressor speed and suction pressure.

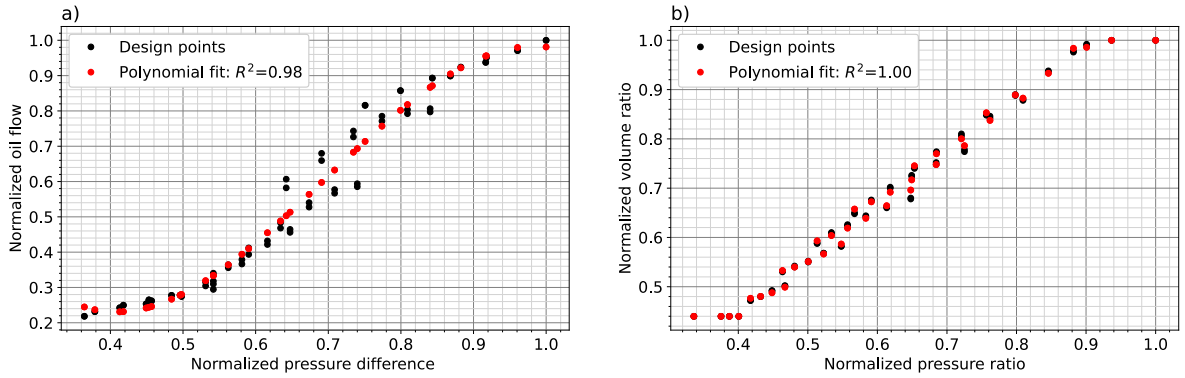

Fig. 6. Comparison of model and design data for a) normalized oil flow as function of normalized pressure difference and b) normalized volume ratio as function of normalized pressure ratio for the screw compressor.

As with the various heat exchangers, the screw compressor was fitted in relation to the design data based on a virtual test bench. The screw compressor model was fitted in relation to refrigerant flow, discharge temperature, and compressor power. The result before and after the fit can be seen in Fig. 7.

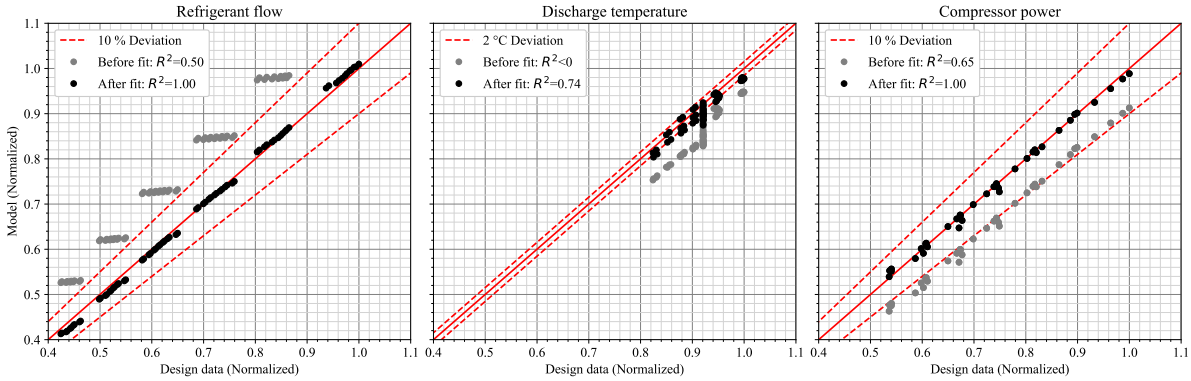

Fig. 7. Refrigerant flow, discharge temperature, and compressor power for the model as a function of the design data.

2.4. System modelling and validation

The heat pump system model was aggregated from the various modelled components and PI-controllers. The P and I gains for the different controllers were tuned by comparison with relevant test data from experiments with the heat pump system including controllers. The experiments were conducted in a controlled test environment with several pressure, temperature, flow rate, and level sensors installed. The media on the source and sink side was water, and the heat was exchanged between the source and sink side in a mixing loop.

To validate the behavior of the system model, the independent input parameters for the model (see Fig. 1) were varied based on three different experimental test cases. The cases defined were:

- Case 0: Test period with relatively stable operating conditions.
- Case 1: First dynamic operating case – variation of receiver level set-point.
- Case 2: Second dynamic operating case – with several simultaneous changes being made in the system at the same time, including gradual change of compressor speed as well as changing inlet water temperatures and flows.

The independent input parameters and results from the three validation cases, including further descriptions of the cases are described in the next section. The three cases were chosen because they illustrated a nuanced view of different operating conditions. Case 0 illustrates the steady state error for the various dependent parameters. Case 1 illustrated what happened when one parameter was changed. And finally, case 2 illustrated what happened to the heat pump when multiple changes were made at the same time. The sampling time for the data was 1 second and all three cases were tested without economizer.

3. Results

For the three cases the model was simulated 10,000 seconds before time = 0 s with the independent input parameters from time = 0 s as inputs. This made the results from the model stable before the input parameters from the data processing stated to change at time = 0 s. In a similar manner the tests of the heat pump were kept in steady state for a period before the start of the logging period.

3.1. Case 0: Stable operating conditions

Case 0 was the baseline case which aimed at verifying that energy- and mass balances for model and test data matched in a steady-state case. The case lasted for around 1300 seconds, and the defined independent input parameters can be seen in Fig. 8. From the figure it can be seen that the operating data for the water inlet temperatures to the evaporator (HX1), sub-cooler (HX4), and oil cooler (HX6), respectively, were relatively stable. The inlet temperature to the oil-cooler and sub-cooler were identical. In addition to this, the water flow and compressor were also relatively stable.

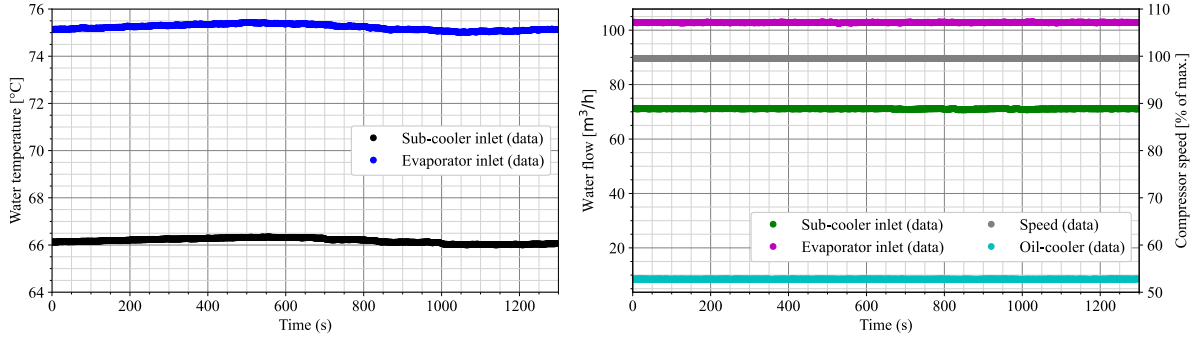

Fig. 8. Independent parameters for case 0 – stable operation.

Fig. 9 shows a log(p)-h diagram and a T-$\dot{Q}$ diagram for case 0 at time = 0 s. The log(p)-h diagram shows the cycle process for both the model and measured data, respectively. The T-$\dot{Q}$ diagram shows the normalized

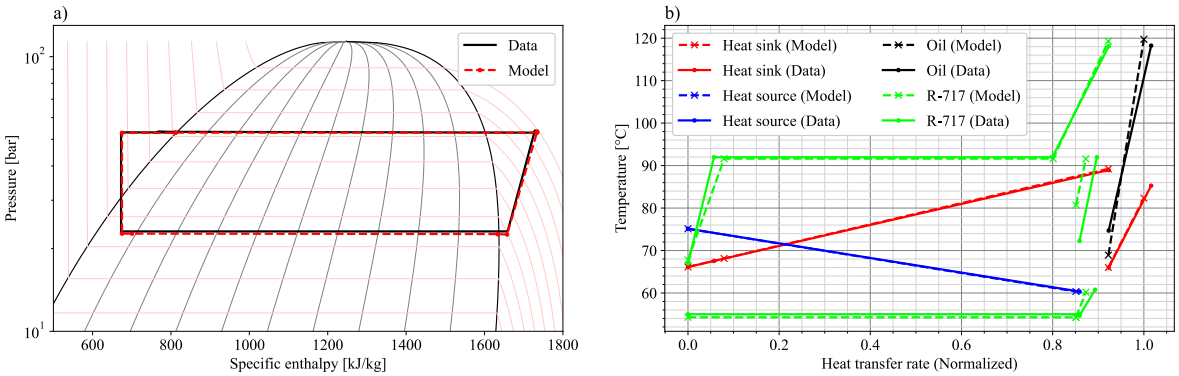

Fig. 9. Case 0 – a) Log(p)-h and b) T-$\dot{Q}$ diagram with comparison of model and test data at time = 0 s.

heat transfer rate (Norm. HTR) for the different heat exchangers on the water, ammonia, and oil side, in relation to the temperature levels. The heat transfer rate for the data was determined from an energy balance using flow and temperature sensors. The heat transfer rate for the oil cooler (HX6) was in parallel with the heat transfer rate from the sub-cooler and the condenser on the water side.

The temperatures and heat transfer rates were generally in good agreement between model and measured data for case 0. The difference between model and test data for selected values can be seen in Table 1.

Table 1. Difference between model and test data at time = 0 s for selected values.

	Data	Simulation	Deviation
Evaporation temperature [°C]	55.00	54.28	0.72 K
Condensing temperature [°C]	91.96	91.62	0.34 K
Discharge temperature [°C]	118.09	119.27	-1.18 K
Sub-cooler outlet temperature [°C]	66.98	67.80	-0.82 K
Superheating before compressor [K]	5.77	6.18	0.41 K
Outlet temperature - water sink [°C]	88.95	89.24	0.29 K
Norm. HTR – water sink [%]	92.28	92.22	0.06 %
Norm. HTR – water source [%]	89.30	87.27	2.03 %
Norm. HTR – oil-cooler [%]	9.32	7.78	1.54 %

The dynamic response of some of the key parameters for case 0 can be seen Fig. 10. Here the discharge pressures (a), evaporation temperature (b), and the oil inlet temperature (c) are shown as a function of time. In this case there were no major differences between measured data and model. It can be seen that for all three parameters the model generally follows the data with an offset of approximately 0.5 bar for the discharge pressure, 0.7 K for the evaporating temperature and 0.1 K for the oil inlet temperature to the compressor (first 700 s).

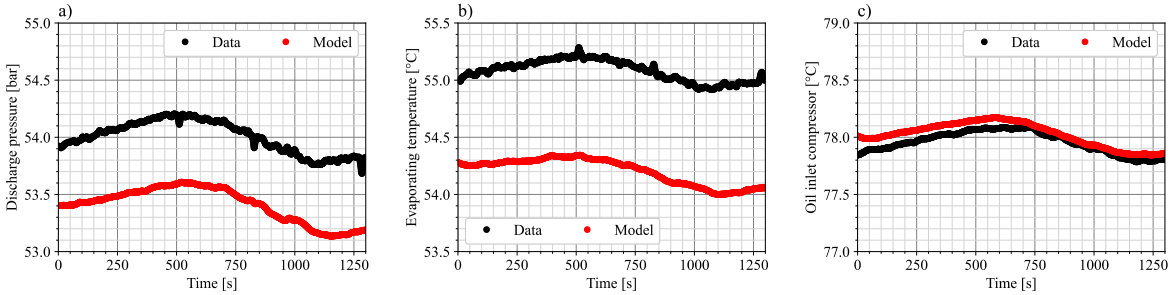

Fig. 10. Dynamic response for a) discharge pressure, b) evaporating temperature, and c) oil temperature in case 0.

3.2. Case 1: Set-point change for the receiver level

Case 1 was a controlled dynamic test, where the system and hereby the independent parameters were kept in steady state until 412 seconds after the defined start of case 1, as seen in Fig. 11. At that time a single set point change of the high-pressure control valve was made, and the level in the receiver was lowered. The change of

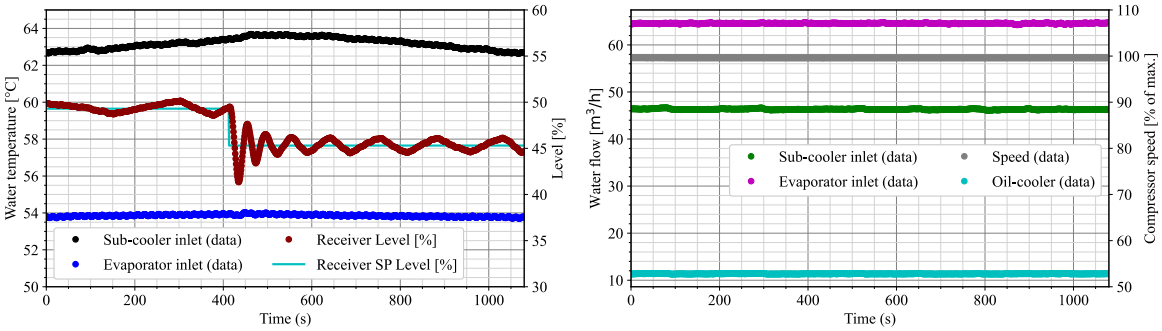

Fig. 11. Independent input parameters for case 1 – change in receiver level.

level was estimated to correspond to a 7.3 % change of the fraction for the liquid volume in the receiver from 54.5 % down to 47.2 % based on a level measurement in the cylindrical formed receiver with horizontal orientation. After the set-point change in the receiver the other input parameters for e.g. the compressor speed and secondary flows on the sink and source side continued to be almost the same.

Fig. 12 shows the influence and the dynamic response for the heat pump system with the change in receiver for both the test data and simulation results. In Fig. 12 (a) the filling level is shown, and it can be seen that for both the test data and the dynamic model the value for the filling level was within the neutral zone (± 1 % of set-point with deactivated PI controller) for the controller before the set-point change. Immediately after the set-point change the level oscillates similarly outside the neutral zone for both the test data and the model before being within the neutral zone again around 150 seconds after the change. Inside the neutral zone the PI-controller in the model was creating a higher oscillating frequency compared to the test data.

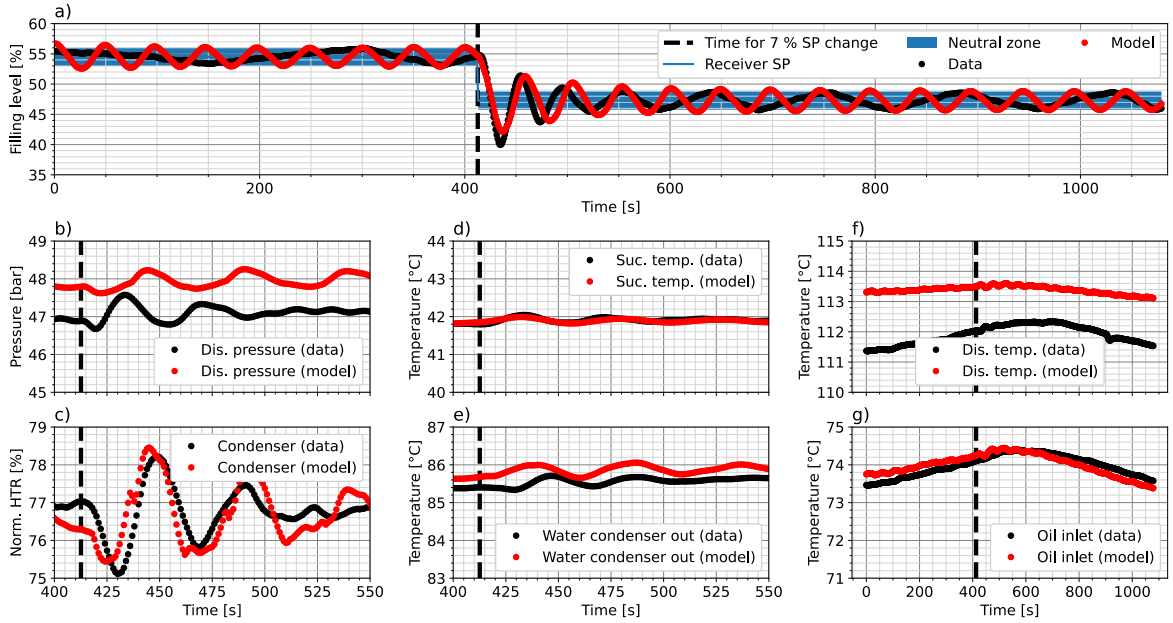

Fig. 12. Comparison of dynamic response in case 1 between data and model for a) the filling level for R1, b) discharge pressure, c) normalized heat transfer rate for the condenser, d) suction temperature, e) temperature for water out of condenser, f) discharge temperature, and g) oil inlet temperature.

Fig. 12 further shows the discharge pressure (b), normalized heat transfer rate for the condenser (c), suction temperature (d), temperature for water outlet of condenser (e), discharge temperature (f), and oil inlet temperature (g) for the dynamic response in case 1. The control of the receiver liquid level has a considerable impact on the dynamic response in the system. The rapid decrease of the set point of the liquid level in R1 immediately caused a small pressure increase on the suction side and subsequently on the discharge side of the compressor. It can be seen that the dynamic response for the outlet pressure was a little slower for the model than for the test data, while the dynamic response for the water outlet temperature from the condenser was a bit faster for the model compared to the test data.

One of the challenges about the system model was to replicate the various controls in the heat pump. For example, the thermostatic valve (V7) in the oil circuit was relatively slow regulating in relation to the set point, which in this case was defined as 73.5 °C, see Fig. 12(g). In the model, this thermostatic valve was modeled with a PI regulator, which then had to reflect the measured data. Another control parameter was the high-pressure control of the liquid level in the receiver. The liquid level was controlled by a PI regulator which was active outside a neutral zone. In order to find the PI gains (proportional gain, k, and the time constant of the integrator block, T_i) that reflected the measured data, a parameter sweep was made to find the best combination. Fig. 13 shows some of the investigated PI gains. The parameters shown for the red curve were used for further work with the model. For this combination of PI gains, it was possible to control the level within the neutral zone before the set-point change, and it had the same characteristics for the overshoot immediately following the set-point change. In addition, a corresponding settlement time of around 150 seconds occurred before the level again was inside the neutral zone.

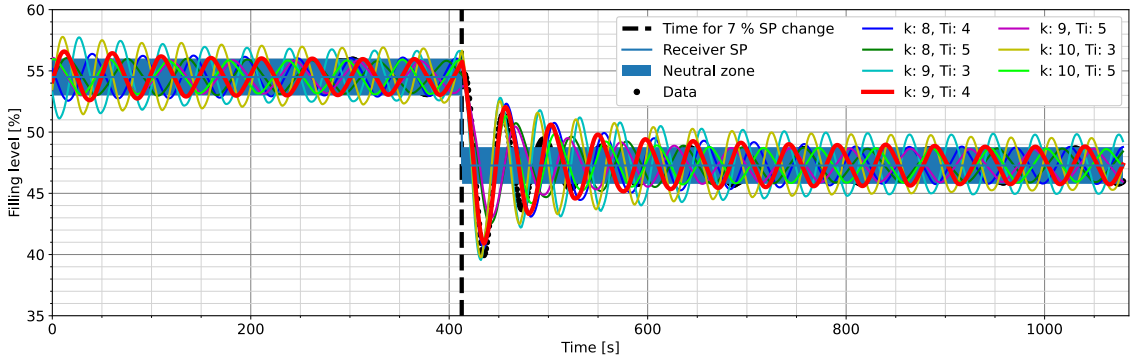

Fig. 13. Different PI gains for the controller for liquid level in receiver R1.

3.3. Case 2: Multiple simultaneous changes

Fig. 14 shows multiple dynamic variations of the independent input parameters for case 2. The graph on the left side shows the inlet temperatures to the evaporator and the sub-cooler which were similar to the inlet temperature for the oil-cooler. The graph on the right shows the water flows for the sub-cooler, evaporator, oil-cooler and the compressor speed, respectively. In this case the inlet water temperatures varied by 2 K to 3 K during the 2500 seconds of the case, and the water flows were increased as the compressor speed was gradually increased from 3060 RPM to 3580 RPM.

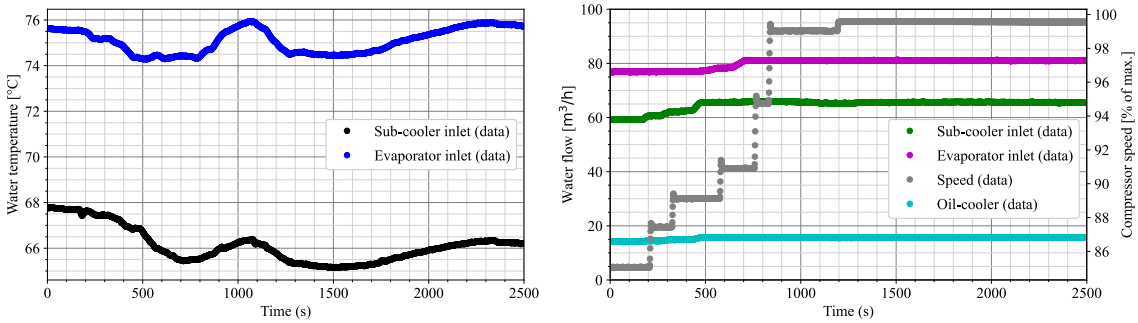

Fig. 14. Independent parameters for case 2 – multiple simultaneous changes.

Although there were several different parameters that were changed at the same time, case 2 still gave a good indication of the ability for the model to predict the dynamic response of the heat pump. Fig. 15 shows the influence and dynamic response of the heat pump system with changes in RPM and inlet water temperatures for both the test data and simulation results.

Fig. 15(a) shows the discharge pressure as a function of time. In addition, the six times with an RPM increase as well as the water inlet temperature to the sub-cooler are highlighted. The model was able to predict a discharge pressure which captures the dynamic fluctuation from the water inlet temperature and changes in RPM. Fig. 15 also shows the dynamic response of normalized heat transfer rate for oil-cooler (b) and condenser (c) as well as the suction temperature (d), water outlet temperature (e) of the condenser, discharge temperature (f), and oil inlet temperature to the compressor (g). In general, there was a good correlation between dynamic patterns in the test data and the model. The model discharge pressure (a) was on average 0.56 bar higher at RPM below 3580, while the average difference at full speed was 0.25 bar. With each RPM change, the pressure level for the test data and the simulation changes. The new pressure levels of the measurements were achieved approximately twice as fast as in the model, but with the same pressure increase. The difference in the normalized heat transfer rate for oil cooling (b) and condensing (e) were on average 1.2 % and 0.7 % lower for the model compared to the measured data. The suction temperature (d) was on average 0.04 °C lower for the model. Here, however, there were a few sudden drops in measured data that the model did not capture. The modelled discharge temperature (d) was on average 2 °C above the measured data, however with a similar dynamic response. The modelled water outlet temperature of the condenser (f) and oil inlet temperature to the compressor were on average 0.2 °C and 0.3 °C above the measured data. For the temperature out of the condenser the dynamic response was similar between the data and simulated values, while for the oil inlet temperature dynamic response also was similar, however with smaller deviation occurring around 1500 seconds.

The dynamic response for the normalized heat transfer rate for the oil cooler was also similar between data and simulated values, however at full load there was an offset of approximately 1.1 %.

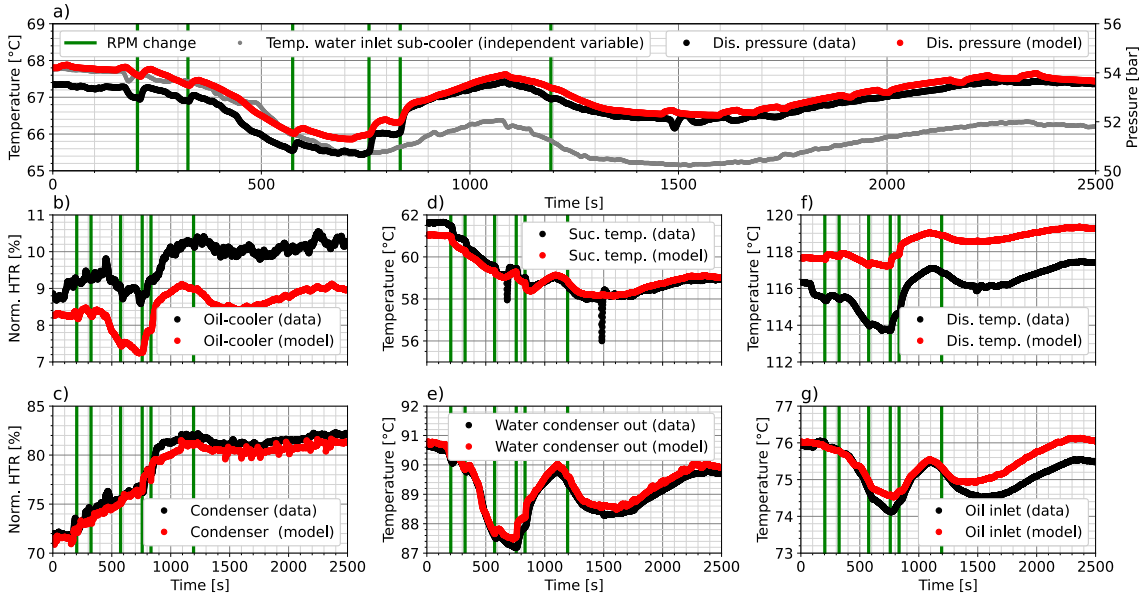

Fig. 15. Comparison of dynamic response in case 2 between data and model for a) the discharge pressure, b) heat transfer rate for oil-cooler, c) heat transfer rate for the condenser, d) suction temperature, e) temperature for the water outlet of the condenser, f) discharge temperature, and g) and oil inlet temperature.

4. Discussion

The validation of the results from the simulation model compared to the test data showed that the model was able to satisfactorily predict the dynamics seen during operation of the heat pump system. This would not be likely to be captured with only quasi-stationary models as also discussed in [24]. The offset difference between the experimental data and the model in relation to the steady state error can for example be attributed to small differences in the fitted parameters (design data in relation to experimental data), not modeled physical aspects, and/or measurement uncertainties. The difference for the dynamic aspects can for example be attributed to the PI controllers.

The validation showed the importance of suitable parameters used in the controllers. Especially the control of the expansion valve (V7) was sensitive for the system operation. In order to tune and validate the controllers further, more tests are suggested where set-point changes are introduced one at a time. These suggested tests including a test program with ramping the compressor speed up and down, on/off operation with the economizer, changing the capacity glider position, changing the sink and source side flow and temperature, while maintaining all other independent input parameters constant. Since there are several different PI-controllers with different PI-gains and neutral zones which simultaneously influencing each other, future structured tests will further show if additional changes to the PI-controllers in the model are necessary.

In some cases, the dynamic response for the simulation model showed shorter settling times with lower amplitude compared to the measured data. This might be due to neglecting pipe connections between the components and the corresponding heat- and pressure losses. If these connections were taken into account a minor contribution to the dynamic response for the model is expected, however it is also expected that the model will be numerically stiffer and has an accordingly higher computation time [8].

For case 1, in which a change of the liquid level in the receiver was imposed, another source of error could be due to a difference in the interpretation of the value of the experimental data for the height measurement in the horizontal receiver. The measured value in the test data was a relative height measurement, while the used filling level in Dymola was the fraction between the volume of liquid and the total volume. The conversion from the relative height measurement to the filling level was based on approximated values. In future work the exact position of the sensor will be investigated in order to precisely compare the receiver fluid level in the measurements and the simulation.

In some cases, the controllers in the physical heat pump use a varying proportional band depending on the difference between the desired set-point value and the actual value. If the error signal is large and outside the proportional band the controller ramps up quicker, while the controller is slower for low error signals. Further

studies are needed to investigate if this effect needs to be included in the model in order to further minimize errors between the dynamic model and the measured data.

In the present study, the heat pump was modeled without details of the components for the secondary streams, which determines the sink and source inlet water temperatures and flows. These were defined by the test setup, and then used as inputs to the model. This approach is suitable for validation of the heat pump system model. In future studies, it may be favorable to also include the modelling of pumps and valves on the secondary sides when investigating holistic control procedures to accommodate fast changes of external parameters.

Several design points have been used to fit the individual components in the system. For most of the parameters, it was possible to fit the design data very well to the individual components. There was, however, a little difference for the discharge temperature of the screw compressor. In order to make this temperature more accurate, further work can be done to incorporate the oil cooling in the model in more detail.

By making a detailed dynamic model and validating the system in different operating conditions, it was possible to get a thoroughly validated model, which then can be used for more in-depth analyses for many different operating conditions. By having a validated model, these analyses can be done much faster compared to full scale testing of the heat pump system in the laboratory. Hence, the presented validated model in this study allows for relatively quick investigation of different control approaches and development of design guidelines in order to be used as a general development tool for large-scale ammonia heat pumps.

5. Conclusion

A dynamic model of a large-scale one-stage ammonia heat pump with a screw compressor and different types of heat exchangers was implemented in Dymola. The model was validated with three different cases: a case with stable operating conditions, a case with a single set-point change for the receiver level, and a case with multiple simultaneous changes. The validation showed a satisfying agreement between the measured data and the model, both in relation to the offset errors and the dynamic response.

The dynamic model was developed by systematically modelling each individual component in the heat pump system, and fitting it mainly against the component design data, before finally combining the components into an overall system model. The different controllers were set up to match the dynamic response for the measured data in order to be able to validate the system model. The various dynamic responses in the model compared to the measured data were highly dependent on the used gains for the PI controllers, but through parameter sweeps of the PI gains it was possible to find values that led to satisfying agreement between the measured data and the model.

Case 0 showed that the model overall in a steady state scenario performed similar to the performance for the measured data. In case 1 the liquid level in the receiver was changed which subsequently led to a change in pressure for the heat pump system which the model captures. For case 1 it was further shown that the dynamic response overall was in good agreement for all the individual components, however also that for a few components small time differences in the dynamic response were observed, which can be refined in future work. Finally, case 2 showed that model and measured data agree well for changes in the temperatures on the sink and source side as well as for fast changes of the compressor speed.

The results from the validation showed that this dynamic system model has great potential to be used for developing holistic control strategies and design guidelines in order to further improve the resilience and performance under fluctuating boundary conditions for large-scale heat pumps.

Acknowledgements

This work was funded by EUDP (Energy Technology Development and Demonstration Programme) under the project ”Development of Fast Regulating Heat Pumps using Dynamic Models” (64020-1077).

References

[1] IEA, “Heat Pumps,” Paris, 2022. [Online]. Available: https://www.iea.org/reports/heat-pumps

[2] J. J. Aguilera, W. Meesenburg, T. Ommen, W. B. Markussen, J. L. Poulsen, B. Zühlsdorf, and B. Elmegaard, “A review of common faults in large-scale heat pumps,” *Renew. Sustain. Energy Rev.*, vol. 168, p. 112826, 2022, doi: 10.1016/j.rser.2022.112826.

[3] B. P. Rasmussen and B. Shenoy, “Dynamic modeling for vapor compression systems-Part II: Simulation tutorial,” *HVAC R Res.*, vol. 18, no. 5, pp. 956–973, 2012, doi:

10.1080/10789669.2011.582917.
[4] P. Li, H. Qiao, Y. Li, J. E. Seem, J. Winkler, and X. Li, "Recent advances in dynamic modeling of HVAC equipment. Part 1: Equipment modeling," *HVAC R Res.*, vol. 20, no. 1, pp. 136–149, 2014, doi: 10.1080/10789669.2013.836877.
[5] P. Li, Y. Li, J. E. Seem, H. Qiao, X. Li, and J. Winkler, "Recent advances in dynamic modeling of HVAC equipment. Part 2: Modelica-based modeling," *HVAC R Res.*, vol. 20, no. 1, pp. 150–161, 2014, doi: 10.1080/10789669.2013.836876.
[6] Modelica Association, "Modelica Libraries — Modelica Association," 2019.
[7] M. Gräber, K. Kosowski, C. Richter, and W. Tegethoff, "Modelling of heat pumps with an object-oriented model library for thermodynamic systems," *Math. Comput. Model. Dyn. Syst.*, vol. 16, no. 3, pp. 195–209, 2010, doi: 10.1080/13873954.2010.506799.
[8] W. Meesenburg, W. B. Markussen, T. Ommen, and B. Elmegaard, "Optimizing control of two-stage ammonia heat pump for fast regulation of power uptake," *Appl. Energy*, vol. 271, no. December 2019, p. 115126, 2020, doi: 10.1016/j.apenergy.2020.115126.
[9] W. Meesenburg, T. Ommen, W. B. Markussen, and B. Elmegaard, "Influence of component sizing on the dynamic behaviour of fast-regulating two-stage ammonia heat pumps," *ECOS 2020 - Proc. 33rd Int. Conf. Effic. Cost, Optim. Simul. Environ. Impact Energy Syst.*, pp. 923–934, 2020.
[10] J. L. Poulsen, J. Joaquín, A. Schulte, S. Försterling, W. Meesenburg, J. Koehler, B. Elmegaard, and B. Zühlsdorf, "Model-based analysis of a heat pump cascade system using seawater and ammonia as working fluids," *35th Int. Conf. Effic. Cost, Optim. Simul. Environ. Impact Energy Syst.*, 2022.
[11] W. Meesenburg, J. Joaquín, R. Kofler, and W. B. Markussen, "Prediction of fouling in sewage water heat pump for predictive maintenance," 2022.
[12] Dassault Systemes, "Dymola 2022 - Dynamic Modeling Laboratory." Dassault Systèmes.
[13] "TIL 3.9 - Model library for thermal components and systems." TLK Thermo GmbH, 2022.
[14] Modelica-Association, "Modelica and the Modelica Standard Library." 2021. [Online]. Available: http://www.modelica.org
[15] M. W and V. H, *An Introduction to Computational Fluid Dynamics - The Finite Volume Method*. Pearson Education (Us), 2007.
[16] TLK-Thermo, "ModelFitter." 2022. [Online]. Available: http://www.tlk-thermo.de
[17] X. Tao and C. A. Infante Ferreira, "Heat transfer and frictional pressure drop during condensation in plate heat exchangers: Assessment of correlations and a new method," *Int. J. Heat Mass Transf.*, vol. 135, pp. 996–1012, 2019, doi: 10.1016/j.ijheatmasstransfer.2019.01.132.
[18] H. Martin, "A theoretical approach to predict the performance of chevron-type plate heat exchangers," *Chem. Eng. Process. Process Intensif.*, vol. 35, no. 4, pp. 301–310, 1996, doi: 10.1016/0255-2701(95)04129-X.
[19] R. L. Amalfi, F. Vakili-Farahani, and J. R. Thome, "Flow boiling and frictional pressure gradients in plate heat exchangers. Part 2: Comparison of literature methods to database and new prediction methods," *Int. J. Refrig.*, vol. 61, pp. 185–203, 2016, doi: 10.1016/j.ijrefrig.2015.07.009.
[20] G. A. Longo, S. Mancin, G. Righetti, and C. Zilio, "A new model for refrigerant boiling inside Brazed Plate Heat Exchangers (BPHEs)," *Int. J. Heat Mass Transf.*, vol. 91, pp. 144–149, 2015, doi: 10.1016/j.ijheatmasstransfer.2015.07.078.
[21] Modelica-Association, "Functional Mock-up Interface," 2022. https://fmi-standard.org/ (accessed Mar. 21, 2022).
[22] TLK-Thermo, "Model development of physical based screw compressor with injection." Braunschweig, 2021.
[23] P. Kurzweil, B. Frenzel, and F. Gebhard, *Physik Formelsammlung*. 2008.
[24] H. Biglarian, M. Abbaspour, and M. H. Saidi, "Evaluation of a transient borehole heat exchanger model in dynamic simulation of a ground source heat pump system," *Energy*, vol. 147, pp. 81–93, Mar. 2018, doi: 10.1016/J.ENERGY.2018.01.031.